Molecular Genetics and Genomics (2019) 294:773–787
https://doi.org/10.1007/s00438-019-01547-x

ORIGINAL ARTICLE

Genotype–phenotype correlation and expansion of orodental anomalies in *LTBP3*-related disorders

Narin Intarak[1] · Thanakorn Theerapanon[1] · Sermporn Thaweesapphithak[2] · Kanya Suphapeetiporn[3,4] · Thantrira Porntaveetus[1] · Vorasuk Shotelersuk[3,4]

Received: 21 October 2018 / Accepted: 8 March 2019 / Published online: 18 March 2019

Abstract

The latent transforming growth factor-beta-binding protein 3 (*LTBP3*), encoding extracellular matrix proteins, plays a role in skeletal formation. Mutations in *LTBP3* have been associated with various types of skeletal dysplasia. We aimed to characterize clinical and molecular features of more patients with mutations in the gene, which may help suggest genotype–phenotype correlation. The first two East Asian patients with short stature, heart defects, and orodental anomalies having *LTBP3* mutations were identified. Whole exome and Sanger sequencing revealed that the one with a novel heterozygous missense (c.2017G>T, p.Gly673Cys) mutation in *LTBP3* had clinical features consistent with acromicric dysplasia (ACMICD). The variant was located in the highly conserved EGF-like calcium-binding domain adjacent to the single reported *LTBP3* variant associated with ACMICD. This finding supports that *LTBP3* is a disease gene for ACMICD. Another patient with a novel homozygous splice site acceptor (c.1721-2A>G) mutation in *LTBP3* was affected with dental anomalies and short stature (DASS). Previously undescribed orodental features included multiple unerupted teeth, high-arched palate, and microstomia found in our patient with ACMICD, and extensive dental infection, condensing osteitis, and deviated alveolar bone formation in our patient with DASS. Our results and comprehensive reviews suggest a genotype–phenotype correlation: biallelic loss-of-function mutations cause DASS, monoallelic missense gain-of-function mutations in the EGF-like domain cause ACMICD, and monoallelic missense gain-of-function mutations with more drastic effects on the protein functions cause geleophysic dysplasia (GPHYSD3). In summary, we expand the phenotypic and genotypic spectra of *LTBP3*-related disorders, support that *LTBP3* is a disease gene for ACMICD, and propose the genotype–phenotype correlation of *LTBP3* mutations.

Keywords Acromicric dysplasia · Acromelic dysplasia · Amelogenesis imperfecta · Oligodontia · Skeletal dysplasia · Cardiac anomalies

Introduction

LTBP is a group of extracellular proteins involved in regulation of TGF-β activity and microfibrillar network. LTBPs comprise four LTBP isoforms (LTBP-1, -2, -3, and -4) and contain several compartments including epidermal growth factor (EGF), 4-Cys, hybrid, and calcium binding

Communicated by Stefan Hohmann.

Electronic supplementary material The online version of this article (https://doi.org/10.1007/s00438-019-01547-x) contains supplementary material, which is available to authorized users.

✉ Thantrira Porntaveetus
thantrira.p@chula.ac.th

[1] Genomics and Precision Dentistry Research Unit, Department of Physiology, Faculty of Dentistry, Chulalongkorn University, Bangkok 10330, Thailand

[2] Center of Excellence for Regenerative Dentistry, Faculty of Dentistry, Chulalongkorn University, Bangkok 10330, Thailand

[3] Center of Excellence for Medical Genomics, Department of Pediatrics, Faculty of Medicine, Chulalongkorn University, Bangkok 10330, Thailand

[4] Excellence Center for Medical Genetics, King Chulalongkorn Memorial Hospital, The Thai Red Cross Society, Bangkok 10330, Thailand

EGF domains that are interspersed with TGFβ-binding domains (Robertson et al. 2015). The *LTBP3* encodes the latent TGF-β binding protein 3 which is the extracellular matrix protein required for osteoclast function and microfibril biology (Zilberberg et al. 2012). Mutations in *LTBP3* have been associated with several human disorders including acromicric dysplasia (ACMICD; OMIM #102370), geleophysic dysplasia3 (GPHYSD3; OMIM #617809), and dental anomalies and short stature (DASS; OMIM #601216). To date, the relationship between *LTBP3* mutations and these diverse anomalies has not been verified. The purpose of this study was to identify more patients with mutations in the gene and characterize their clinical features, which may help suggest genotype–phenotype correlation.

ACMICD and GPHYSD3 belong to the acromelic dysplasia group of genetically heterogeneous skeletal dysplasias characterized by short stature, brachydactyly, progressive joint limitation, and delayed bone age (Faivre et al. 2001; Le Goff et al. 2011). Clinical features of GPHYSD3 consist of full 'happy' face including full cheek, small nose with anteverted nares, broad nasal bridge, and thin upper lip with flat philtrum, hepatomegaly, tracheal stenosis, and progressive cardiac valvular thickening which often leads to early death (Le Goff et al. 2011; McInerney-Leo et al. 2016). Distinct from GPHYSD3, ACMICD shows mild facial features without progressive cardiac and respiratory problems (Le Goff et al. 2011; McInerney-Leo et al. 2016).

DASS is characterized by short stature, brachyolmia, and hypoplastic amelogenesis imperfecta. Oligodontia, thoracic aortic aneuryms and dissection, and mitral valve prolapse were frequently observed in DASS (Dugan et al. 2015; Guo et al. 2018).

To our knowledge, only one *LTBP3* mutation has been identified in ACMICD, two in GPHYSD3, and eight in dental anomalies and short stature (DASS; OMIM #601216). A heterozygous missense mutation was previously identified in a family with autosomal dominant ACMICD. Two de novo heterozygous, stop-loss and donor splice site, variants were found in two unrelated patients with the dominant GPHYSD3 (McInerney-Leo et al. 2016). Biallelic *LTBP3* mutations were reported in patients with autosomal recessive DASS (Dugan et al. 2015; Guo et al. 2018; Huckert et al. 2015; Noor et al. 2009).

In this study, we investigated phenotype and genotype of two unrelated Thai patients affected with ACMICD and DASS. Exome and sanger sequencings were performed to identify pathogenic variants. Our analyses expanded clinical and mutational spectra and propose genotype–phenotype correlation in *LTBP3*-related disorders.

Materials and methods

Enrollment of human subjects

Two Thai families were recruited for genetic studies of skeletal dysplasia. Thorough examinations and blood collection were performed after obtaining the written informed consent from each participant. The study was approved by the Institutional Review Board, Chulalongkorn University (IRB 470/61) and performed according to the ethical standards of the 1964 Declaration of Helsinki and its later amendments or comparable ethical standards.

Micro computerized tomography (CT) analysis

The lower left third molar of patient 1 was surgically removed and subjected for scanning with specimen μCT 35 (SCANCO Medical, Brüttisellen, Switzerland) and the Image Processing Language (IPL, Scanco Medical AG) at the Mineralized Tissue Research Unit at the Faculty of Dentistry, Chulalongkorn University. The mineral density of dental hard tissues was quantified compared with the controls using the same tooth type.

Whole exome sequencing (WES) and bioinformatics

The genomic DNA was extracted from peripheral blood leukocytes. The DNA samples and sequencing data were processed as previously described (Porntaveetus et al. 2017). WES was done at Macrogen, Inc. (Seoul, Korea) using VariantStudio™ version 3.0.12 (Illumina, Inc., USA). All variants were filtered using the following criteria: (1) quality score ≥ 20, (2) read depth ≥ 10, (3) location in or close to the coding regions, (4) < 1% minor allele frequency in the database of Exome Variant Server, Exome Aggregation Consortium (ExAC), 1000 Genomes Project Consortium, dbSNPs, and in-house database of 1,400 Thai exomes. The variants were termed novel if they were not present in the Human Gene Mutation Database (http://www.hgmd.cf.ac.uk/ac/index.php) and the Genome Aggregation Database (gnomAD) (Lek et al. 2016). Alignment of conserved regions among species including *Homo sapiens* (NP_001123616.1), *Mus musculus* (NP_032546.2), *Monodelphis domestica* (XP_007502752.1), *Empidonax traillii* (XP_027763522.1), *Danio rerio* (NP_001244070.1), and *Anolis carolinensis* (XP_016854597.1) was performed by Clustal Omega (version 1.2.4). Analysis of three-dimensional protein structures was established using the PyMOL Molecular Graphics System, Version 2.0 Schrödinger, LLC (Schrodinger 2015).

Mutation validation

The Sanger sequencing was performed to confirm the mutations detected by WES. The coding region of *LTBP3* was amplified by *LTBP3*-specific primers: LTBP3_1_F:CTT CTCAGATGTGAACGAGTGC and LTBP3_2_R:TCC CCTCACCTTCGCACA. The splice site acceptor (SSA) region of *LTBP3* was amplified by *LTBP3* specific primers: LTBP3_3_F: GAAGCGTCGTTATCTGGGGT and LTBP3_4_R: CTGGAGTTGGAGTATGGGCG. PCR products were sent for Sanger sequencing at Macrogen, Inc. (Seoul, Korea).

Results

Phenotypic characterization

Patient 1 is the only son of non-consanguineous healthy Thai parents (Fig. 1a). He was delivered by C-section due to cephalopelvic disproportion with a birth weight of 4000 g (1.8 SD) and a birth length of 55 cm (2 SD). He was referred to our hospital at the age of 10 years and 2 months due to severe short stature. His height was 116.7 cm (< − 3 SD) and weight was 22.7 kg (− 1.8 SD). The height of his

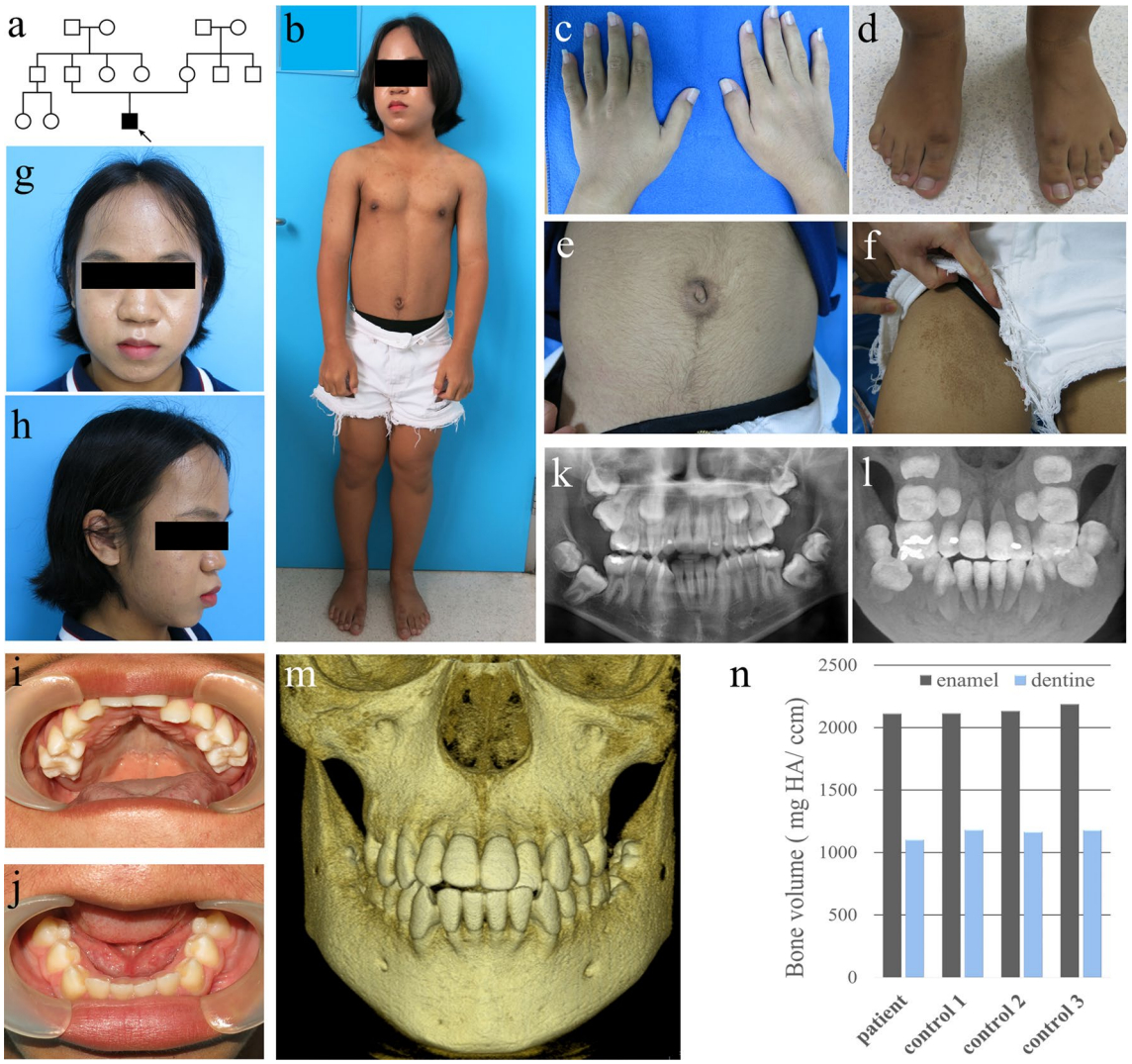

Fig. 1 The pedigree of family 1 and characteristics of the proband. The proband is indicated by an arrow. A filled symbol represents an affected family member. **a** Family pedigree. The proband at age of 18 years and 11 months showed short stature (**b**), short hands, feet, fingers, and toes (**c, d**). The periumbilical skin was darkened (**e**). Hyperpigmentation was observed on his right thigh (**f**). His facial features consisted of a round face, well-defined eyebrows, bulbous nose, long philtrum, and thickened lips (**g, h**). Oral examinations revealed high arched palate and 22 permanent teeth (**i, j**). Panoramic radiograph and computerized tomography exhibited unerupted upper second premolars and all second and third molars (**k, l**). The erupted teeth had unremarkable appearance (**m**). Micro-CT analysis detected the hydroxyapatites (HA) levels of the proband's enamel and dentine was comparable to those of the controls (**n**)

father was 170 cm and his mother was 165 cm. Physical examinations of the proband showed short stature, short limbs, hands, and feet, and mild bowed legs (Fig. 1b–d). Hyperpigmentation was observed on his right thigh and umbilical skin (Fig. 1e, f). His liver, spleen, kidneys and eyes were unremarkable. His upper body height was 60 cm, lower body height was 56 cm (1.3 SD) (Turan et al. 2005), and arm span was 110 cm (< − 3 SD) (Zhu et al. 2015). He had Tanner stage I and normal intelligence. His facial characteristics showed round face, well-defined eyebrows, bulbous nose, broad and depressed nasal bridge, long philtrum, and thickened lips (Fig. 1g, h). Clinical oral examination showed microstomia, tooth crowding, high arched palate, and only 22 permanent teeth (Fig. 1i, j). Radiographically, multiple impacted teeth including upper second premolars and all second and third molars were present. The unerupted upper teeth were highly embedded in the maxilla (Fig. 1k, l). Computerized tomography scan revealed normal shape and texture of erupted teeth (Fig. 1m). His impacted teeth were surgically removed at the age of 16 years and 10 months. The hydroxyapatite contents of enamel and dentine of the patient's lower left third molar were similar to those of the controls (Fig. 1n), suggesting that the mineral density of dental hard tissues was not affected.

Skeletal survey, at the age of 10 years and 2 months, demonstrated short extremities, mild lumbar lordosis, and shortened tubular bones of the hands (Fig. 2a–e). The cone-shaped epiphyses, external notch on the 2nd metacarpals, and internal notch on the 5th metacarpals were not observed. His bone age was 9 years old. The levels of thyroxine (9.18 pg/dL; 5.5–12.1 pg/dL) and thyroid stimulating hormone (2.35 mIU/L; 0.64–6.27 mIU/L) were within normal limits. Echocardiogram revealed mild valvular aortic stenosis. He was prescribed amlodipine and had regular checkups. At 11 years of age, the patient had adenotonsillar hypertrophy with obstructive sleep apnea. The oxygen desaturation was significantly declined. He was diagnosed with chronic hypoxemic hypertension with mild restrictive lung condition. After adenotonsillectomy, his breathing and oxygen level were improved. At the age of 18 years and 11 months, the patient demonstrated limited extension of his shoulders, elbows and knees, and high pitch voice. Radiographic findings showed

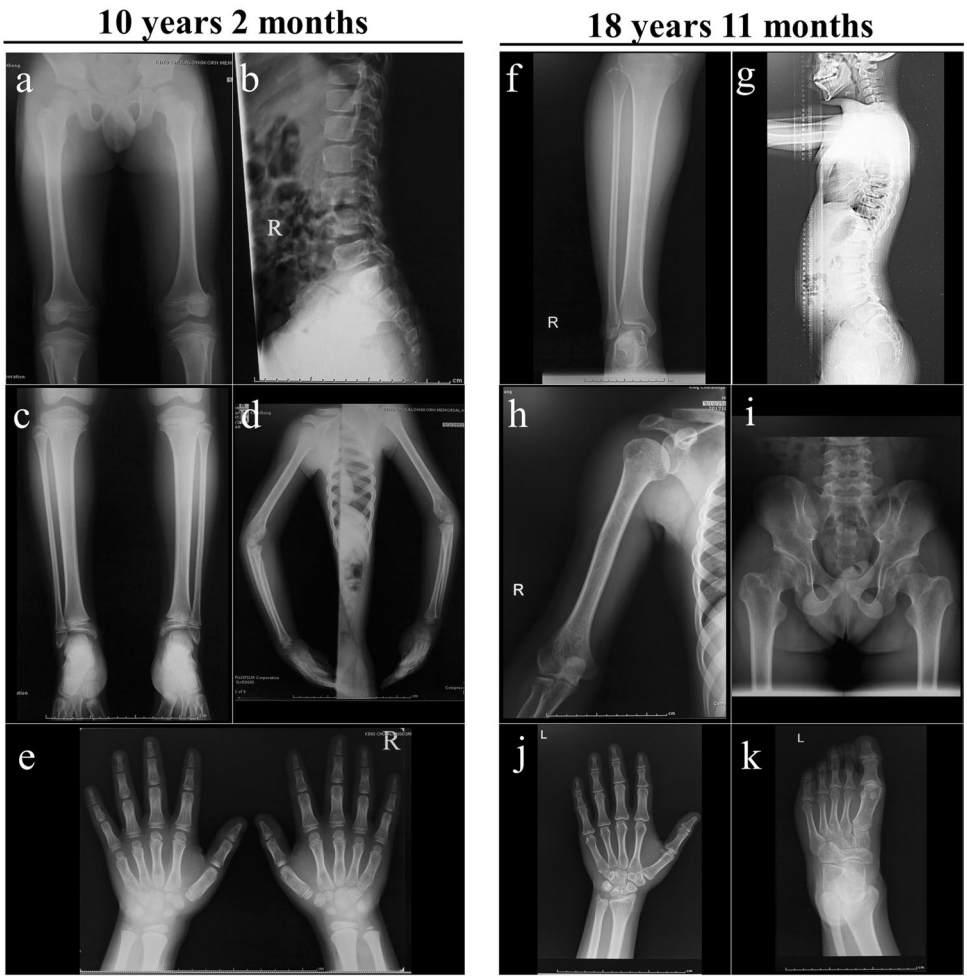

Fig. 2 Radiographic findings of the patient 1 at the age of 10 years and 2 months presented with short long bones and phalangeal bones, and mild lumbar lordosis (**a**–**e**). At the age of 18 years and 11 months, he had mild hallux valgus and lumbar lordosis (**f**–**k**). **a** femur, **b, g** spine, **c, f** tibia and fibula, **d, h** humerus, radius, ulna, **e, j** hand, **i** pelvic, **k** foot

progressive lumbar lordosis, short metacarpals, and mild hallux valgus (Fig. 2f–k). His upper body was 72.5 cm; lower body 70 cm (1.5 SD) (Turan et al. 2005); arm span 136 cm (< −3 SD); hand length 16 cm (−2.5 SD) (Guerra et al. 2014); and middle finger 6.5 cm (−3 SD) (Rastogi et al. 2009). He had Tanner stage 5. His cardiac condition was stable.

Patient 2 was a 24-year-old Thai female who was born with congenital heart defects to consanguineous healthy parents (Fig. 3a). She presented short stature and scoliosis. Her height was 140 cm (< −2.7 SD). The heights of her father and mother were 170 cm (at the median) and 165 cm (0.8 SD), respectively. Her facial feature showed bulbous nose, thick eyebrows, and long philtrum (Fig. 3b, c). Oral examination revealed yellowish and small teeth, hypoplastic enamel, severe destructive crown exposing the dentine and dental pulp, multiple retained roots, widely spaced arch, and resorbed mandibular alveolar ridge (Fig. 3d–f). She had never had tooth extraction or any dental pain. Radiographic findings include thin enamel with reduced radiopacity, irregular alveolar bone level, and extensive bone infection with condensing osteitis (Fig. 1g). The dental features suggest hypoplastic amelogenesis imperfecta. Her intellectual development was normal. The proband's siblings and parents were healthy and did not have dental anomalies.

Mutation analyses

For patient 1, the variants passed the filtering criteria were screened using the lists of genes associated with short stature (Supplementary Table 1). Two missense variants passed the criteria (Supplementary Table 2). They were in *LTBP3* and *PLEC*, previously known to be associated with skeletal dysplasia and epidermolysis bullosa simplex, respectively. Since the patient had skeletal dysplasia, we therefore focused on the one in *LTBP3*. It is a heterozygous missense mutation, c.2017G>T (p.Gly673Cys) in exon 14 of *LTBP3* (NM_001130144.2). Mutations in this gene have been reported in patients with acromicric dysplasia, which was consistent with the patient's characteristics. The p.Gly673Cys was predicted to be deleterious (SIFT, 0) (Ng and Henikoff 2003), probably damaging (PolyPhen-2 score, 0.999) (Adzhubei et al. 2010), and possibly pathogenic (M-CAP score, 0.450) (Jagadeesh et al. 2016). The amino acid changed from glycine to cysteine at position 673 situated within a calcium-binding EGF-like domain (Fig. 4c, d). It was highly conserved in various species including human, mouse, opossum, bird, chameleon, and frog (Fig. 4e). Visualization of the predicted 3-D structure of LTBP3 suggested that the mutant residue was bigger, more hydrophobic, and less flexible than the wild type. The mutation was expected to disturb the calcium

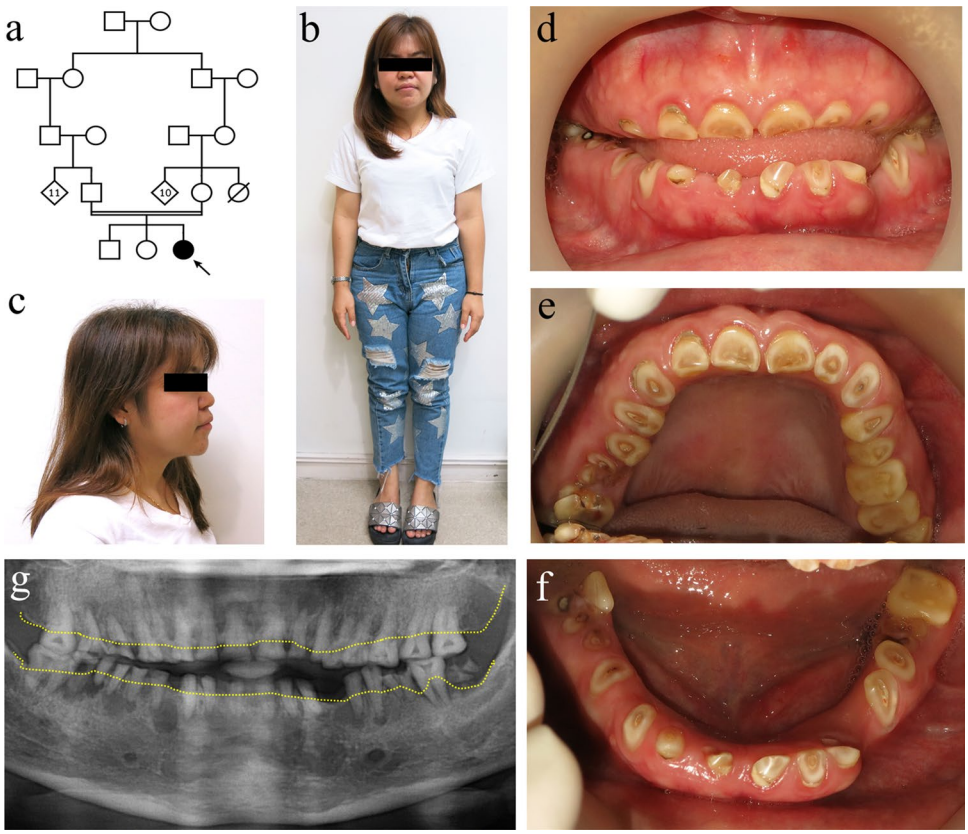

Fig. 3 The pedigree of Family 2 and characteristics of the proband. **a** Family pedigree. **b, c** The proband at age of 24 years showed short stature. Her facial features presented bulbous nose and long philtrum. **d–f** Oral examination revealed severe destructive dentition, yellowish hypoplastic enamel, several retained roots, and resorbed mandibular alveolar ridge. **g** The panoramic radiograph showed that the enamel had reduced radiopacity similar to the dentine. Several infections in the jaw bones with condensing osteitis were detected. The level of alveolar bone was irregular indicated by yellow dotted line. (Color figure online)

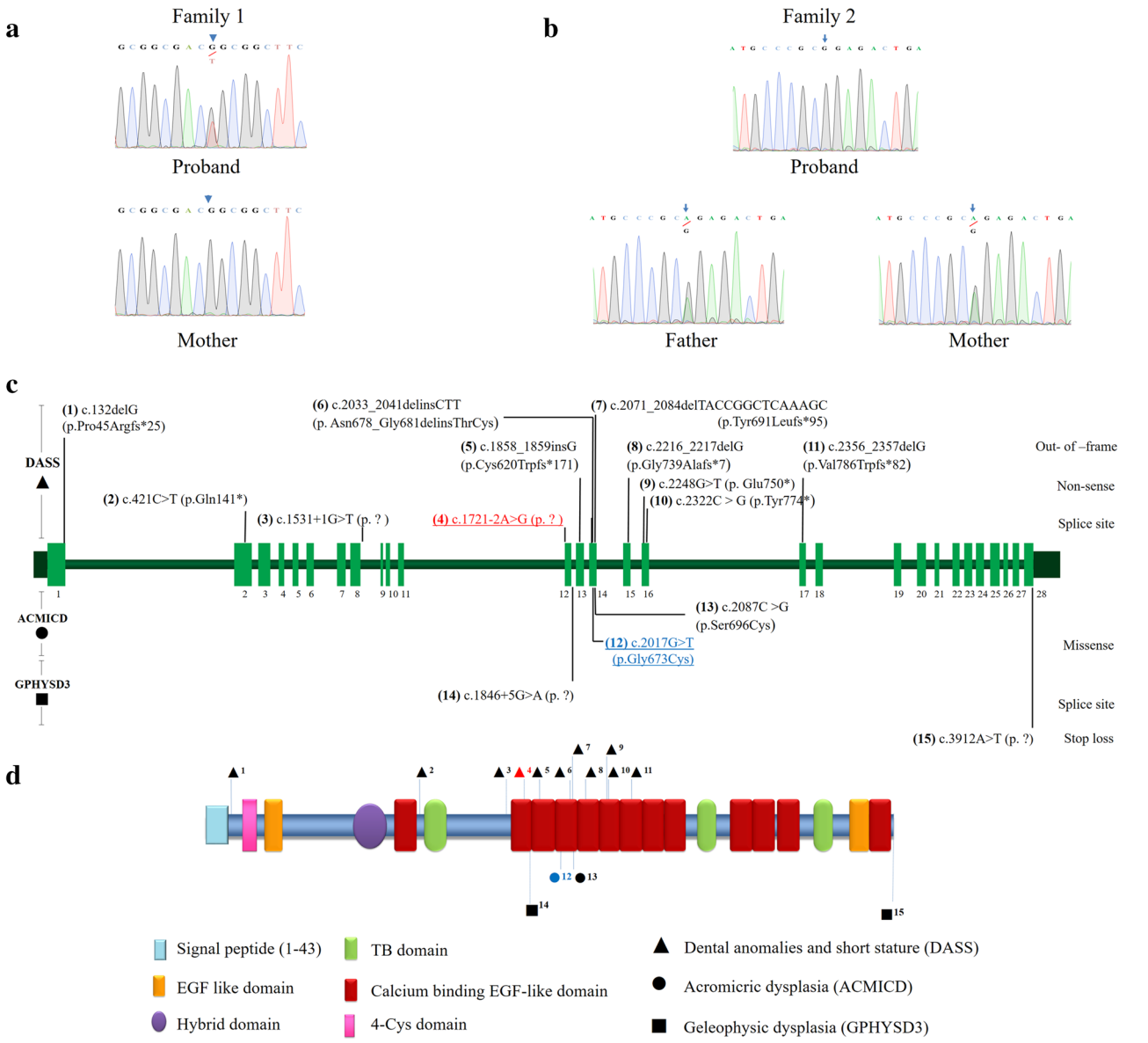

binding domain, produce an unusual angle of backbone conformation, and impact protein function (Venselaar et al. 2010) (Fig. 4f). This variant was not observed in his mother (Fig. 4a). The proband's biological father's blood was not available. The mutation has never been previously described.

For patient 2, we performed trio-based WES analyses. The variants identified are shown in Supplementary Table 3. A novel homozygous splice site mutation, c.1721-2A>G, in splice site acceptor (SSA) region before exon 12 of *LTBP3* matched with the patient's features of dental anomalies and short stature (DASS). Her parents were heterozygous for the

◂**Fig. 4** Genetic analyses. **a** Sequence chromatograms illustrated the heterozygous missense mutation, c.2017G>T (p.Gly673Cys) in the *LTBP3* gene (NM_001130144.2) in patient 1, which is absent in his mother. **b** Sequence chromatograms showed the homozygous splice site mutation, c.1721-2A>G in SSA region of *LTBP3* in patient 2, which is present in the heterozygous form in the parents. **c, d** Schematic diagrams of the *LTBP3* gene and structural domains of LTBP3 proteins. The identified mutations were indicated above (DASS, triangle) and under (ACMICD, circle and GPHYSD3, square) the exons of the gene and structural domains of the protein. The mutation identified in this study was underlined. **e** Sequence alignment of partial amino acid sequences of LTBP3 protein among human and different species. Conservation of the codon 673 of LTBP3 across species was covered by a box. **f** Three-dimensional diagram showed the change of glycine (red color) to cysteine (yellow color) at amino acid residua 673 in the EGF-like domain (green colour) of LTBP3. Differences in size and structure were observed between wild-type and mutant. EGF-like domain, epidermal growth factor like domain; TB domain, transforming growth factor β-binding protein-like domain. The mutations numbered 1, 6, 9 were identified in Guo et al. (2018); 2, 3, 7, 8, 11 in Huckert et al. (2015); 5 in Dugan et al. (2015); 10 in Noor et al. (2009); 13, 14, 15 in McInerney-Leo et al. (2016); and 4, 12 in our study. (Color figure online)

mutation (Fig. 4b–d). The splice site mutation was expected to alter the acceptor site causing pre-mRNA splicing and exon skipping which could result in nonsense-mediated mRNA decay (Hug et al. 2016; Nagy and Maquat 1998).

Discussion

In this study, we identified the first two East Asian patients having *LTBP3* mutations expanding phenotypic and genotypic spectrum of *LTBP3*-related disorders. Our first proband had typical ACMICD features including short stature, brachydactyly, short limbs, limited joint extension, and dysmorphic facial features without hepatomegaly and respiratory/cardiac involvements. Multiple unerupted teeth, high-arched palate, and microstomia were observed, suggesting the disturbance of orodental structure. However, the mineral density of the teeth was not affected. To date, a single missense mutation in *LTBP3* has been reported in ACMICD (McInerney-Leo et al. 2016). We identified a novel heterozygous missense mutation, c.2017G>T (p.Gly673Cys) in *LTBP3* associated with ACMICD. This finding strongly supports the causative role of *LTBP3* for ACMICD. Several lines of evidences showed that p.Gly673Cys was pathogenic. First, it was absent in HGMD, gnomAD, and our in-house exome databases. Second, in silico analyses demonstrated that the p.Gly673Cys was damaging and pathogenic. Third, the introduction of cysteine in place of glycine which is the most flexible amino acid resulted in the bigger size, more hydrophobicity, and less flexibility of the mutant protein compared to the wild type (Fig. 4f). These could alter conformation and function of LTBP3. Importantly, the mutation was located in the EGF-like calcium-binding domain and highly conserved in several species. Previous mutations particularly anchored to this EGF-like domain were shown to disrupt LTBP3 levels resulting in aortic or cardiac defects (Dugan et al. 2015; Guo et al. 2018; McInerney-Leo et al. 2016). The Cys may specifically result in intra- or inter-molecule disulfide bonds so that another missense mutation in the EGF-like calcium domain may have a different effect. Of note, the missense mutation of our patient was located adjacent to a single reported missense variant in the EGF-like calcium-binding domain of LTBP3 associated with ACMICD, supporting a genotype–phenotype correlation.

Our patient with DASS was found to harbor the homozygous splice site acceptor mutation, c.1721-2A>G, in *LTBP3*. The change of sequence from "CAG" to "CGG" at constitutive acceptor splice site in the intron 12 of *LTBP3* gene was expected to alter the constitutive SSA causing an exon skipping or intron retention (Mora et al. 2014; Souma et al. 2016; Verselis et al. 2000). These could result in nonsense-mediated mRNA decay and reduced protein levels (Hug et al. 2016; Nagy and Maquat 1998).

DASS is caused by homozygous or compound heterozygous mutations in *LTBP3*. It is characterized by short stature, brachyolmia, and hypoplastic amelogenesis imperfecta showing inter- and intrafamilial variability (Huckert et al. 2015). Some DASS patients exhibited tooth agenesis or oligodontia (Dugan et al. 2015; Noor et al. 2009). It was also proposed that homozygous *LTBP3* variants could predispose individuals to later onset of thoracic aortic aneurysms and dissections, along with skeletal and dental anomalies (Guo et al. 2018). The enlarged aortic root and ascending aorta were observed in *Ltbp3*$^{-/-}$ mice (Guo et al. 2018). The *LTBP3* was expressed in several tissues including heart, bone, and teeth (Huckert et al. 2015). These suggest that *LTBP3* mutations could result in a broad range of phenotypes.

A comprehensive summary of all reported disorders with *LTBP3* mutations is demonstrated in Table 1 and Fig. 4c, d. We observed that biallelic loss-of-function mutations including splice site, out-of-frame, and nonsense mutations were particularly found in "DASS" while monoallelic missense gain-of-function or dominant negative mutations in the highly conserved EGF-like calcium-binding domain were associated with "ACMICD" and monoallelic stop-loss or splicing mutations with "GPHYSD3". Majority of DASS parents who harbored monoallelic hypomorphic *LTBP3* mutations were healthy and did not have dental anomalies, indicating haplosufficiency and that one normal allele of LTBP3 is sufficient for normal development. Contrarily, the monoallelic *LTBP3* mutations causing ACMICD or GPHYSD3 could be either gain-of-function (hypermorphic) or dominant negative effects (antimorphic). These propose that different modes of inheritance and natures of *LTBP3* mutations contribute to different syndromes. Further,

Table 1 Phenotypic spectrum associated with *LTBP3* mutations

	This study		McInerney-Leo et al. (2016)					Guo et al. (2018)		
	AD	DASS	AD			GD1	GD2	DASS		
General information										
Age (year/month)	18/9	24/0	48/0[a]	18/0[a]	12/0[a]	0/11	1/2	54/0[b]	55/0[b]	59/0[b]
Gender	M	F	M	M	M	M	M	M	F	F
Number of affected individuals studied in the family	1	1	3			1	1	3		
Ethnic	Thai	Thai		Caucasian		Caucasian	Caucasian	American		
Parental consanguinity	No	Yes	No			No	No	No		
Height (cm (SD))	142.5 (< −3.0 SD)	140.0 (−2.7 SD)	128.0 (−5.6 SD)	139.0 (−5.4 SD)	120.0 (−4.0 SD)	60.5 (< −3.0 SD)	65.5 (< −3.0 SD)	160 (−2.2 SD)	152 (−1.7 SD)	147 (−2.5 SD)
AD and GD shared features										
Short stature	+	+	+	+	+	+	+	+	+	+
Brachydactyly	+	NA	+	+	+	+	+	NA	NA	NA
Delayed bone age	+	NA	NA	NA	NA	+	+	NA	NA	NA
Pseudomuscular build	NA	NA	+	+	+	+	+	NA	NA	NA
Cone-shaped epiphyses	−	NA	NA	NA	NA	−	+	NA	NA	NA
Restricted joint mobility	+	NA	+	+	+	+	+	NA	NA	NA
Round face	+	−	+	+	+	+	+	NA	NA	NA
Long philtrum	+	+	NA	NA	NA	+	−	NA	NA	NA
AD specific features										
Bulbous nose	+	+	+	+	+	−	−	NA	NA	NA
Microstomia	+	−	−	−	−	−	−	NA	NA	NA
Thickened lips	+	−	NA	NA	NA	±	±	NA	NA	NA
Well-defined eyebrows	+	+	+	+	+	−	−	NA	NA	NA
External notch on the 2nd metacarpals (childhood)	−	NA	+	+	+	−	−	NA	NA	NA

Table 1 (continued)

	This study		McInerney-Leo et al. (2016)					Guo et al. (2018)		
	AD	DASS	AD			GD1	GD2	DASS		
Internal notch on the 5th metacarpals (childhood)	−	NA	+	+	+	−	−	NA	NA	NA
Hoarse voice	−	NA	+	+	+	−	−	NA	NA	NA
GD specific features										
Small nose with anteverted nares	−	−	−	Anteverted nares only	−	+	+	NA	NA	NA
Broad and depressed nasal bridge	+	+	−	±	−	NA	NA	NA	NA	NA
Thin upper lip	−	−	−	−	−	−	−	NA	NA	NA
Progressive cardiac valvular thickening	−	−	−	−	−	−	−	−	−	−
Respiratory compromise	+	−	+	−	+	+	+	−	−	−
Laryngotracheal stenosis	−	−	+	+	−	+	+	−	−	−
Hepatomegaly	−	−	−	−	−	+	+	−	−	−
Early death due to cardiac and/or respiratory disease	−	−	−	−	−	+	+	−	−	−
DASS specific features										
Tooth missing	−	−	NA	NA	NA	NA	NA	NA	NA	NA
Retarded teeth eruption	−	−	NA	NA	NA	NA	NA	NA	NA	NA
Amelogenesis imperfecta	−	+	NA	NA	NA	NA	NA	+	+	+
Osteopenia	−	NA	NA	NA	NA	NA	NA	−	−	+
Mild mitral valve prolapse	+	?	−	−	+	−	−	−	+	+

Table 1 (continued)

	This study		McInerney-Leo et al. (2016)					Guo et al. (2018)		
	AD	DASS	AD			GD1	GD2	DASS		
Thoracic aortic aneurysms/dissections	–	–	–	–	–	–	–	+	+	–
Scoliosis	–	+	NA	NA	NA	NA	NA	–	–	+
Other clinical finding										
Arachnodactyly	–	N/A	NA	NA	NA	NA	NA	NA	NA	NA
Acanthosis nigricans	–	NA	NA	NA	NA	NA	NA	NA	NA	NA
Hypertrichosis	–	NA	NA	NA	NA	NA	NA	NA	NA	NA
Swan necking of the fingers	–	NA	NA	NA	NA	NA	NA	NA	NA	NA
Platyspondyly	–	NA	NA	NA	NA	NA	NA	NA	NA	NA
Triangular face	–	–	NA	NA	NA	NA	NA	NA	NA	NA
Myopia	–	–	NA	NA	NA	NA	NA	NA	NA	NA
Narrow thorax with prominent sternum	–	–	NA	NA	NA	NA	NA	NA	NA	NA
Causative mutation										
Gene	*LTBP3*	*LTBP3*	*LTBP3*	*LTBP3*	*LTBP3*	*LTBP3*	*LTBP3*	*LTBP3*	*LTBP3*	*LTBP3*
Exon	14	splice site acceptor before exon 12	14	14	14	28	Donor splice site after exon 12	1/ 16	1/ 16	1/ 16
Mutation										
DNA	c.2017G>T	c.1721-2A>G	c.2087C>G	c.2087C>G	c.2087C>G	c.3912A>T	c.1846+5G>A	c.132delG, c.2248G>T	c.132delG, c.2248G>T	c.132delG, c.2248G>T
Protein	Gly673Cys	?	Ser696Cys	Ser696Cys	Ser696Cys	1304*Cysext*12	?	Pro45Argfs*25/Glu750*	Pro45Argfs*25/Glu750*	Pro45Argfs*25/Glu750*
Protein domain	EGF-like calcium-binding domain	–	EGF-like calcium-binding domain	EGF-like calcium-binding domain	EGF-like calcium-binding domain	–	–	EGF-like calcium-binding domain	EGF-like calcium-binding domain	EGF-like calcium-binding domain
Mode of transmission										
Inheritance patterns	AD*	AR*	AD*	AD*	AD*	AD*	AD*	AR* compound heterozygous	AR* compound heterozygous	AR* compound heterozygous

Table 1 (continued)

	Guo et al. (2018)		Huckert et al. (2015)					Dugan et al. (2015)		Noor et al. (2009)
	DASS									
General information										
Age (year/month)	44/0[c]	58/0[c]	14/0	13/0[d]	5/6[d]	11/0	16/0, 9/0, 12/0	18/2[e]	15/3[e]	30/0
Gender	M	F	F	F	M	M	F, F, M	F	F	M
Number of affected individuals studied in the family	2		2	2		1	3	2		4
Ethnic	American		Turkey	Caucasian French		Brazil	Pakistan	Emirati		Pakistan
Parental consanguinity	Yes		Yes	No		Yes	Yes	No		Yes
Height [cm (SD)]	160 (−2.3 SD)	150 (−2.0 SD)	140.0 (−4.2 SD)	149.0 (−1.5 SD)	101.0 (−3.0 SD)	128.0 (−3.0 SD)	(−2.0 to −5.0 SD)	136 (−4.2 SD)	132.9 (−4.6 SD)	149.9 (−3.7 SD)
AD and GD shared features										
Short stature	+	+	+	+	+	+	+	+	+	+
Brachydactyly	NA	NA	−	+	+	NA	NA	±	±	−
Delayed bone age	NA	NA	−	NA	NA	NA	NA	NA	NA	NA
Pseudomuscular build	NA	NA	NA	NA	NA	NA	NA	NA	NA	NA
Cone-shaped epiphyses	NA	NA	−	NA	NA	NA	NA	NA	NA	−
Restricted joint mobility	NA	NA	NA	+	NA	NA	NA	NA	NA	NA
Round face	NA	NA	NA	−	−	NA	NA	NA	NA	NA
Long philtrum	NA	NA	NA	NA	NA	NA	NA	NA	NA	NA
AD specific features										
Bulbous nose	NA	NA	NA	NA	NA	NA	NA	NA	NA	NA
Microstomia	NA	NA	NA	NA	NA	NA	NA	NA	NA	NA
Thickened lips	NA	NA	NA	NA	NA	NA	NA	NA	NA	NA
Well-defined eyebrows	NA	NA	+	NA	NA	NA	NA	NA	NA	NA
External notch on the 2nd metacarpals (childhood)	NA	NA	−	NA	NA	NA	NA	NA	NA	NA

Table 1 (continued)

	Guo et al. (2018)		Huckert et al. (2015)					Dugan et al. (2015)		Noor et al. (2009)
	DASS									
Internal notch on the 5th metacarpals (childhood)	NA	NA	–	NA	NA	NA	NA	NA	NA	NA
Hoarse voice	NA	NA	NA	NA	NA	NA	NA	+	+	NA
GD specific features										
Small nose with anteverted nares	NA	NA	NA	NA	NA	NA	NA	NA	NA	NA
Broad and depressed nasal bridge	NA	NA	NA	NA	NA	NA	NA	NA	NA	NA
Thin upper lip	NA	NA	NA	NA	NA	NA	NA	NA	NA	NA
Progressive cardiac valvular thickening	–	–	NA	NA	NA	NA	NA	–	–	NA
Respiratory compromise	–	–	NA	NA	NA	NA	NA	NA	NA	NA
Laryngotra-cheal stenosis	–	–	NA	NA	NA	NA	NA	NA	NA	NA
Hepatomegaly	–	–	NA	NA	NA	NA	NA	NA	NA	NA
Early death due to cardiac and/or respiratory disease	–	–	–	–	–	–	–	–	–	–
DASS specific features										
Tooth missing	NA	NA	NA	NA	NA	NA	+	+	+	+
Retarded teeth eruption	NA	NA	NA	NA	NA	+	NA	+	+	NA
Amelogenesis imperfecta	+	+	+	+	+	+	+	NA	NA	NA
Osteopenia	–	+	+	NA	NA	NA	+	NA	NA	–
Mild mitral valve pro-lapse	–	+	NA	NA	NA	NA	NA	+	–	NA

Table 1 (continued)

	Guo et al. (2018)		Huckert et al. (2015)					Dugan et al. (2015)		Noor et al. (2009)
	DASS									
Thoracic aortic aneurysms/dissections	+	+	NA	NA	NA	NA	NA	NA	NA	NA
Scoliosis	−	+	+	NA	NA	+	+	+	+	+
Other clinical finding										
Arachnodactyly	NA	NA	NA	NA	NA	NA	NA	+	−	NA
Acanthosis nigricans	NA	NA	NA	NA	NA	NA	NA	+	−	NA
Hypertrichosis	NA	NA	NA	NA	NA	NA	NA	+	+	NA
Swan necking of the fingers	NA	NA	NA	NA	NA	NA	NA	+	+	NA
Platyspondyly	NA	NA	+	+	NA	+	+	NA	NA	−
Triangular face	NA	NA	NA	+	+	NA	NA	NA	NA	NA
Myopia	NA	NA	+	−	−	NA	NA	NA	NA	NA
Narrow thorax with prominent sternum	NA	NA	NA	NA	+	NA	NA	NA	NA	NA
Causative mutation										
Gene	*LTBP3*	*LTBP3*	*LTBP3*	*LTBP3*	*LTBP3*	*LTBP3*	*LTBP3*	*LTBP3*	*LTBP3*	*LTBP3*
Exon	14	14	14	2/8	2/8	15	17	13	13	16
Mutation										
DNA	c.2033_2041delinsCTT	c.2033_2041delinsCTT	c.2071_2084delTACCGGCTCAAAGC	c.421C>T, c.1531+1G>T	c.421C>T, c.1531+1G>T	c.2216_2217delG	c.2356_2357delG	c.1858_1859insG	c.1858_1859insG	c.2322C>G
Protein	Asn678_Gly681delinsThrCys	Asn678_Gly681delinsThrCys	Tyr691Leufs*95	Gln141*/?	Gln141*/?	Gly739Alafs*7	Val786Trpfs*82	Cys620Trpfs*171	Cys620Trpfs*171	Tyr774*
Protein domain	EGF-like calcium-binding domain	EGF-like calcium-binding domain	EGF-like calcium-binding domain	EGF-like calcium-binding domain/–	EGF-like calcium-binding domain/–	EGF-like calcium-binding domain	EGF-like calcium-binding domain	EGF-like calcium-binding domain	EGF-like calcium-binding domain	EGF-like calcium-binding domain
Mode of transmission										
Inheritance patterns	AR*	AR*	AR*	AR* compound heterozygous	AR* compound heterozygous	AR*	AR*	AR*	AR*	AR*

AD acromicric dysplasia, *GD* geleophysic dysplasia, *DASS* dental anomalies and short stature, *M* male, *F* female, + presence, − absence, ± equivocal, *NA* not available, *AD** autosomal dominant, *AR** autosomal recessive

[a,b,c,d,e]Each letter represents individuals from the same family

ACMICD and GPHYSD3 can be considered the diseases in the same spectrum. While ACMICD is on the milder end, GPHYSD3 is on the more severe end.

Our study expands phenotypic and genotypic spectra of *LTBP3*-associated disorders, supports the etiologic role of *LTBP3* for ACMICD, and proposes for the first time phenotype–genotype correlation of *LTBP3* mutations. This correlation can assist in the diagnostic and prognostic counseling and clinical management of the patients with *LTBP3* related disorders. Further functional studies will be useful to clarify pathomechanism of the disorders in association with *LTBP3* variants.

Acknowledgements This study was supported by the Thailand Research Fund (RSA6280001, DPG6180001), Faculty of Dentistry, Chulalongkorn University (DRF62003), the Chulalongkorn Academic Advancement Into Its Second Century Project, and the Newton Fund. NI is supported by Ratchadapisek Somphot Fund for Postdoctoral Fellowship, Chulalongkorn University. ST is supported by the 100th Anniversary Chulalongkorn University Fund for Doctoral Scholarship and the 90th Anniversary of Chulalongkorn University Fund (Ratchadaphiseksomphot Endowment Fund). We thank Mr. Trakarn Sookthonglarng and Mr Yuttupong Kunchanapruek for blood collection.

Author contributions NI contributed to conception, data analysis, and drafting the manuscript; TT, ST, KS contributed to data analysis and critical revision of the manuscript; VS and TP contributed to data acquisition and analysis, drafting and critical revision of the manuscript. All authors gave final approval and agree to be accountable for all aspects of the work.

Compliance with ethical standards

Conflict of interest Narin Intarak declares that he has no conflict of interest. Thanakorn Theerapanon declares that he has no conflict of interest, Sermporn Thaweesapphithak declares that he has no conflict of interest. Kanya Suphapeetiporn declares that she has no conflict of interest. Thantrira Porntaveetus declares that she has no conflict of interest. Vorasuk Shotelersuk declares that he has no conflict of interest.

Ethical approval All procedures performed in studies involving human participants were in accordance with the ethical standards of the institutional and/or national research committee and with the 1964 Helsinki declaration and its later amendments or comparable ethical standards.

Informed consent Informed consent was obtained from all individual participants included in the study.

References

Adzhubei IA et al (2010) A method and server for predicting damaging missense mutations. Nat Methods 7:248–249. https://doi.org/10.1038/nmeth0410-248

Dugan SL et al (2015) New recessive truncating mutation in LTBP3 in a family with oligodontia, short stature, and mitral valve prolapse. Am J Med Genet A 167:1396–1399. https://doi.org/10.1002/ajmg.a.37049

Faivre L et al (2001) Acromicric dysplasia: long term outcome and evidence of autosomal dominant inheritance. J Med Genet 38:745–749

Guerra RS, Fonseca I, Pichel F, Restivo MT, Amaral TF (2014) Hand length as an alternative measurement of height. Eur J Clin Nutr 68:229–233. https://doi.org/10.1038/ejcn.2013.220

Guo D-c et al (2018) LTBP3 pathogenic variants predispose individuals to thoracic aortic aneurysms and dissections. Am J Hum Genet 102:706–712. https://doi.org/10.1016/j.ajhg.2018.03.002

Huckert M et al (2015) Mutations in the latent TGF-beta binding protein 3 (LTBP3) gene cause brachyolmia with amelogenesis imperfecta. Hum Mol Genet 24:3038–3049. https://doi.org/10.1093/hmg/ddv053

Hug N, Longman D, Caceres JF (2016) Mechanism and regulation of the nonsense-mediated decay pathway. Nucleic Acids Res 44:1483–1495. https://doi.org/10.1093/nar/gkw010

Jagadeesh KA et al (2016) M-CAP eliminates a majority of variants of uncertain significance in clinical exomes at high sensitivity. Nat Genet 48:1581–1586. https://doi.org/10.1038/ng.3703

Le Goff C et al (2011) Mutations in the TGFbeta binding-protein-like domain 5 of FBN1 are responsible for acromicric and geleophysic dysplasias. Am J Hum Genet 89:7–14. https://doi.org/10.1016/j.ajhg.2011.05.012

Lek M et al (2016) Analysis of protein-coding genetic variation in 60,706 humans. Nature 536:285. https://doi.org/10.1038/nature19057

McInerney-Leo AM et al (2016) Mutations in LTBP3 cause acromicric dysplasia and geleophysic dysplasia. J Med Genet 53:457–464. https://doi.org/10.1136/jmedgenet-2015-103647

Mora M et al (2014) New splice site acceptor mutation in AIRE gene in autoimmune polyendocrine syndrome type 1. PLoS One 9:e101616. https://doi.org/10.1371/journal.pone.0101616

Nagy E, Maquat LE (1998) A rule for termination-codon position within intron-containing genes: when nonsense affects RNA abundance. Trends Biochem Sci 23:198–199

Ng PC, Henikoff S (2003) SIFT: Predicting amino acid changes that affect protein function. Nucleic Acids Res 31:3812–3814

Noor A et al (2009) Oligodontia is caused by mutation in LTBP3, the gene encoding latent TGF-beta binding protein 3. Am J Hum Genet 84:519–523. https://doi.org/10.1016/j.ajhg.2009.03.007

Porntaveetus T, Srichomthong C, Ohazama A, Suphapeetiporn K, Shotelersuk V (2017) A novel GJA1 mutation in oculodentodigital dysplasia with extensive loss of enamel. Oral Dis 23:795–800. https://doi.org/10.1111/odi.12663

Rastogi P, Kanchan T, Menezes RG, Yoganarasimha K (2009) Middle finger length—a predictor of stature in the Indian population. Med Sci Law 49:123–126. https://doi.org/10.1258/rsmmsl.49.2.123

Robertson IB, Horiguchi M, Zilberberg L, Dabovic B, Hadjiolova K, Rifkin DB (2015) Latent TGF-β-binding proteins. Matrix Biol 47:44–53. https://doi.org/10.1016/j.matbio.2015.05.005

Schrodinger LLC (2015) The PyMOL Molecular Graphics System, Version 2.0. https://pymol.org/

Souma T et al (2016) Angiopoietin receptor TEK mutations underlie primary congenital glaucoma with variable expressivity. J Clin Investig 126:2575–2587. https://doi.org/10.1172/JCI85830

Turan S, Bereket A, Omar A, Berber M, Ozen A, Bekiroglu N (2005) Upper segment/lower segment ratio and armspan-height difference in healthy Turkish children. Acta Paediatr 94:407–413

Venselaar H, te Beek TA, Kuipers RK, Hekkelman ML, Vriend G (2010) Protein structure analysis of mutations causing inheritable diseases. An e-Science approach with life scientist friendly interfaces. BMC Bioinform 11:548. https://doi.org/10.1186/1471-2105-11-548

Verselis SJ, Rheinwald JG, Fraumeni JF, Li FP (2000) Novel p53 splice site mutations in three families with Li–Fraumeni syndrome. Oncogene 19:4230. https://doi.org/10.1038/sj.onc.1203758

Zilberberg L, Todorovic V, Dabovic B, Horiguchi M, Courousse T, Sakai LY, Rifkin DB (2012) Specificity of latent TGF-β binding protein (LTBP) incorporation into matrix: role of fibrillins and fibronectin. J Cell Physiol 227:3828–3836. https://doi.org/10.1002/jcp.24094

Zhu M, Jiao YH, Xiong F, Xie F, Guo SJ, Cun YS (2015) Analysis of limb segments length and body proportion of southern Chinese children and adolescents. J Paediatr Child Health 51:1164–1171. https://doi.org/10.1111/jpc.12978